

pH-Dependent Spectroscopy of Tetracycline and Its Analogs

Elmer-Rico E. Mojica · Eric Nguyen · Mariya Rozov · Frank V. Bright

Received: 20 January 2014 / Accepted: 23 April 2014 / Published online: 9 May 2014
© Springer Science+Business Media New York 2014

Abstract Tetracyclines (TCs), broad spectrum antibiotics widely used in the prevention and treatment of infectious diseases, are amphoteric molecules containing several ionizable functional groups that exist predominantly as zwitterions at a given pH value. TCs are reported to undergo a wide variety of reactions at different pH values i.e. TCs form to anhydrotetracyclines at low pH, 4-epitetracyclines at pH 3–5 and isotetracyclines at high pH values. The pH-dependent absorbance and emission properties of tetracycline and its 10 analogs (4-epitetracycline, doxycycline, oxytetracycline, chlortetracycline, 4-epichlortetracycline, isochlortetracycline, methacycline, rolitetracycline, minocycline, and demeclocycline) were investigated and reported in this paper. The main focus of the study was on the pH dependent transformation of epichlortetracycline, chlortetracycline and isotetracycline at basic pH. Absorption, emission and time resolved spectroscopy were used to determine the behavior of the three TC derivatives at this condition. Increasing the buffer's ionic concentration leads to faster transformation to iCTC. A pH dependent transformation of CTC to iCTC was observed and the lifetimes of CTC and iCTC were determined to be 3.0 and 5.89 ns respectively. The distribution factor of CTC to iCTC at basic pH was also reported for the first time.

Keywords Tetracycline · Emission · Lifetime · pH

E.-R. E. Mojica (✉) · E. Nguyen · M. Rozov
Department of Chemistry and Physical Sciences, Pace University,
One Pace Plaza, New York, NY 10038, USA
e-mail: emojica@pace.edu

F. V. Bright
Department of Chemistry, Natural Sciences Complex, University at
Buffalo, The State University of New York, Buffalo,
NY 14260-3000, USA

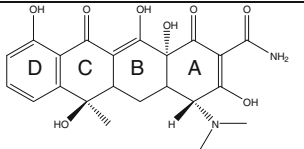
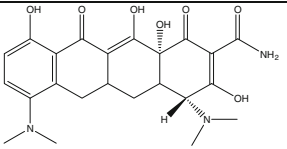
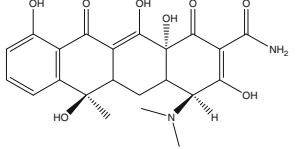
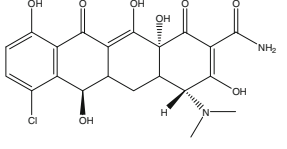
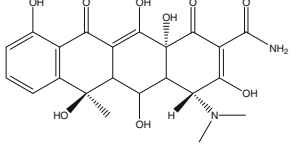
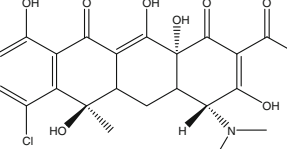
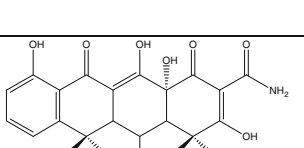
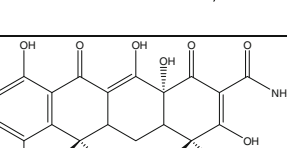
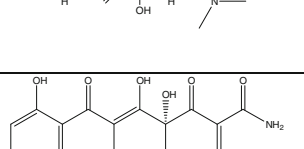
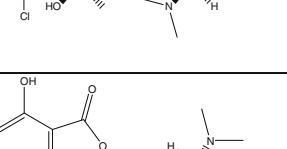
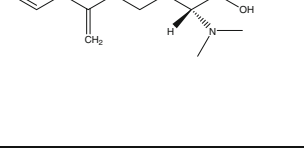
Introduction

Tetracyclines have a general structure known as 1,4,4a,5,5a,6,11,12a-octahydronaphthacene formed by four condensed rings consisting of six carbon atoms each [1] (Table 1). The presence of four intact rings, denoted with letters A, B, C and D, from right to left contributes to the antibiotic activity of tetracycline and its analogs [2, 3]. The basic structure of all TCs includes the amino group joined to ring A, and two systems of keto phenolic chromophores, system A and cycles BCD, which are important for its activity [1]. Alterations of the hydrophobic part of the molecule (from C5 to C9) and modifications of C6 and C7 can give products with greater chemical stability, increased antibiotic activity, and more favorable pharmacokinetics [2]. The various TC analogs differ chiefly by substitution at the C5, C6 and C7 positions on the backbone.

A TC molecule possesses four potentially dissociable protons namely C1–C3 tricarbonyl-methane, C4 dimethyl-amino group and ketophenolic hydroxyl groups on O10 and O12, although only three acidic groups are in the pH region accessible to potentiometric titrations [4–7]. The assignment of dissociation constants to each one of these groups is the subject of controversy and intense studies [4–7]. It was first proposed that pK_{a1} is due to the protonation of oxygen bonded to C3, pK_{a2} is due to protonation of the dimethylamino group and pK_{a3} is due to the protonation of the oxygen atoms to C10 and C12 [4]. However, later studies [6, 8] support the reversal in the assignment of pK_{a2} and pK_{a3} . Table 1 lists the reported and calculated pK_{a} s of the TCs.

There have been several reports on the spectroscopy of TC and its analogs; however, most of the studies deal with tetracycline itself and its interactions with metals and proteins [3, 9–18]. The interactions of chlortetracycline (CTC) with metals [19] and proteins [20, 21] have also been reported.

Table 1 pK_a of TC and its analogs

| Name and pK _a | Chemical Structure | Name and pK _a | Chemical Structure |
|---|---|---|---|
| tetracycline (TC) 3.3, 7.7, 9.5 |  | minocycline (Min) 2.8, 5.0, 7.8, 9.5 |  |
| 4-epitetracycline (ETC) 4.5 ± 1.00 11.02 ± 0.70 |  | demeclocycline (DMC) 3.3, 7.2, 9.3 |  |
| oxytetracycline (OTC) 3.3, 7.3, 9.1 |  | chlortetracycline (CTC) 3.3, 7.4, 9.3 |  |
| doxycycline (DC) 3.4, 7.7, 9.3 |  | epichlortetracycline (ECTC) 4.5 ± 1.00 11.01 ± 0.70 |  |
| methacycline (Met) 3.5, 7.6, 9.2 |  | isochlortetracycline (iCTC) 4.5 ± 1.00 11.01 ± 0.70 |  |
| rolitetracycline (RTC) 7.4 |  | | |

ETC, ECTC and iCTC had no reported pK_a values in literature. Values shown based on calculation by Advanced Chemistry Development (ACD/Labs) Software V8.14

However, most of these studies used pH values above 6. The presence of multiple functional groups makes TCs an amphoteric molecules predominantly existing as zwitterions at a given pH value. pH is one factor that affects the stability of TC in solution [22]. TCs are reported to undergo a wide variety of reactions at different pH values [1].

Epimerization reaction at position C-4 to form epimers is predominantly observed for tetracycline in pH 2 to 6 [23]. Acidic conditions also leads to dehydration of the hydrogen at C5a and the hydroxyl group at C-6 in CTC and its epimer resulting to the formation of anhydrochlortetracycline (ACTC) or 4-epianhydrochlortetracycline (4-EACTC) [24]. At basic conditions, the presence of the hydroxyl group at C-6 allows CTC to readily cleave to form isochlortetracycline (iCTC) [25]. For still unknown reasons, CTC is susceptible to

this transformation at basic pH [26]. A more detailed study on the spectroscopic properties as a function of pH has yet to be reported especially on tetracycline analogs.

In this study, we investigate the pH-dependent absorbance and emission properties of TC and its 10 analogs namely CTC, iCTC, 4-epitetracycline (ETC), doxycycline (DC), oxytetracycline (OTC), methacycline (Met), rolitetracycline (RTC), minocycline (Min), 4-epichlortetracycline (ECTC) and demeclocycline (DMC). This study focuses on the pH-dependent transformation of CTC and iCTC at basic pH by monitoring their spectroscopic properties. The effect of the buffer's ionic concentration on the transformation of CTC to iCTC was also studied. The excited state lifetimes and the distribution factor of CTC and iCTC at basic pH are reported for the first time.

Experimental Section

Chemicals The following reagents were used: tetracycline (>98 %) (Fluka BioChimika); oxytetracycline hydrochloride (OTC) (min 95 % HPLC), doxycycline hyclate (DC),

demeclocycline hydrochloride (DMC), minocycline hydrochloride (Min), rolitetracycline (RTC) and 2-(Cyclohexylamino)ethanesulfonic acid (CHES) (Sigma-Aldrich); chlortetracycline hydrochloride (CTC) (MP Biochemicals, Inc); 4-epitetracycline hydrochloride (ETC)

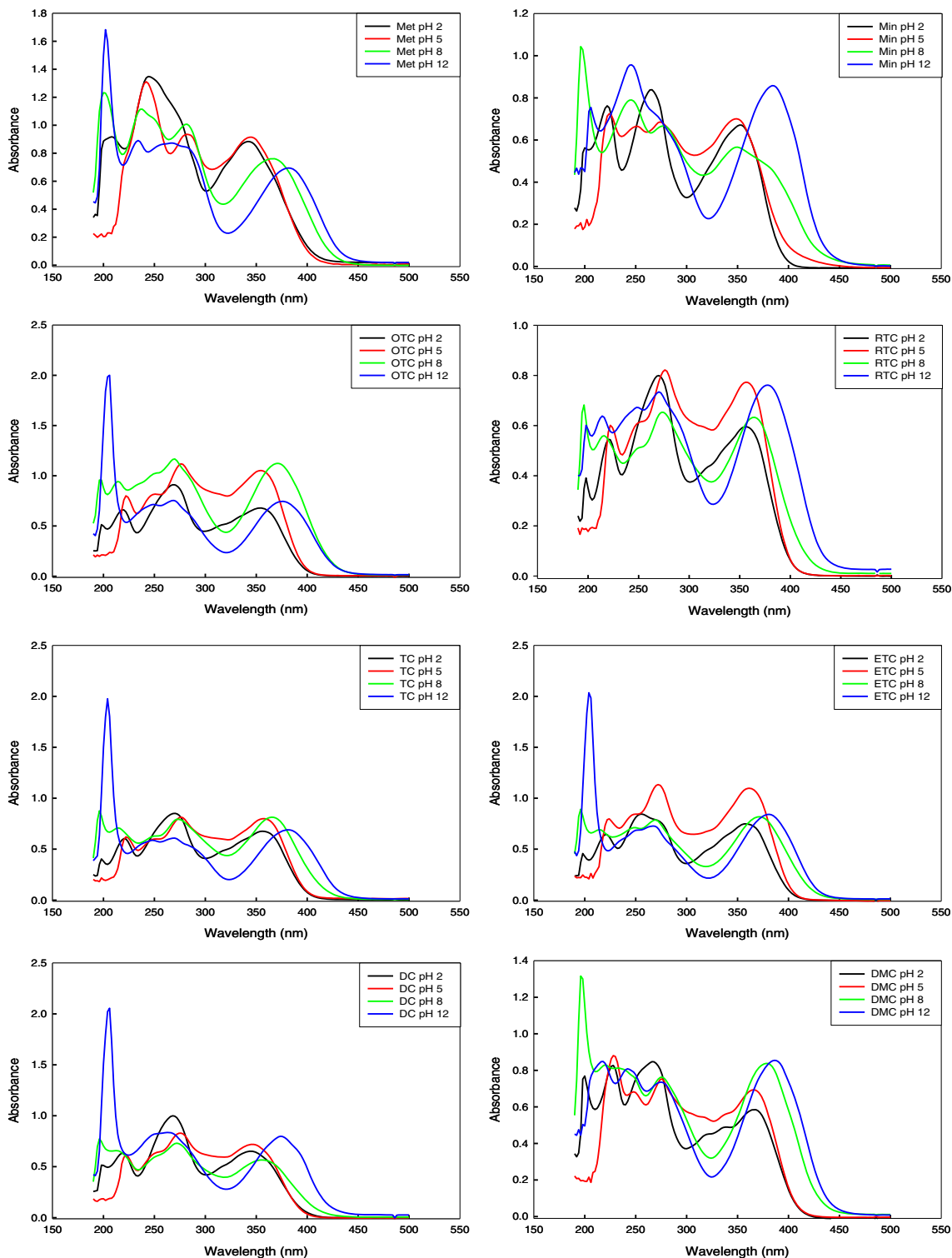


Fig. 1 pH-dependent absorbance spectra of each tetracycline. (TCs in 0.01 M buffer solutions)

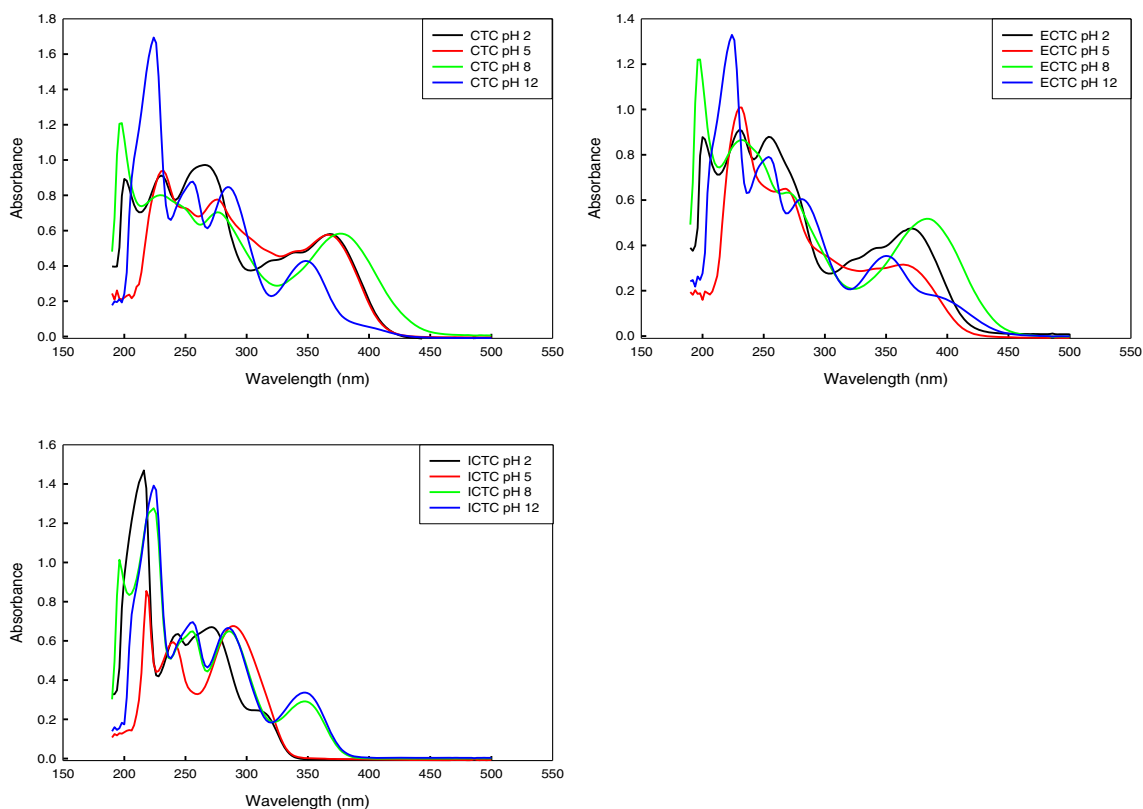


Fig. 2 pH-dependent absorbance spectra of each tetracycline. (TCs in 0.01 M buffer solutions)

(Spectrum); methacycline hydrochloride (Meta) (99.6 % HPLS assay) (Ridel-de-Haen); isochlortetracycline hydrochloride (iCTC), 4-epichlortetracycline (ECTC) and 4-epitetracycline hydrochloride (ETC) (Acros Organics); absolute ethanol (Pharmco-Aaper); sodium hydroxide, sodium phosphate dibasic 7-dihydrate, sodium phosphate monobasic monohydrate, sodium bicarbonate, sodium carbonate and glycine (J.T. Baker) and potassium chloride (Mallinckrodt).

Sample Preparation Aqueous buffer solutions (0.01 M) of different pH (2–12) were prepared using the following buffer systems: glycine-HCl (pH 2–3), citrate buffer (pH 4–6), phosphate buffer (pH 7–8), CHES buffer (pH 9), carbonate-bicarbonate buffer (pH 10), bicarbonate-NaOH (pH 11) and KCl-NaOH (pH 12). The pH was adjusted by adding concentrated HCl or NaOH. Stock solutions of TC and its analogs initially dissolved in ethanol, were diluted with the buffers (50 μ M TC analogs) and immediately analyzed for its absorbance and emission properties. Appropriate blanks were also prepared.

ECTC, CTC and iCTC The excited-state fluorescence lifetimes of three TCs namely, CTC, ECTC and iCTC at basic pH were determined by time correlated single photon counting (TCSPC). The stability of the three TC was

monitored for a month by determining the absorbance within the said period.

Effect of Ionic Strength The effect of buffer's ionic strength (0.001, 0.01 and 0.1 M) in the CTC spectroscopic properties at basic pH was determined. The prepared solution was immediately analyzed for its absorbance and emission properties.

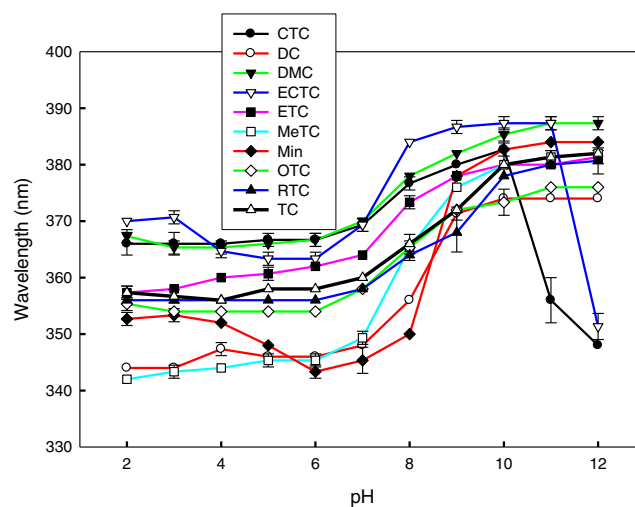
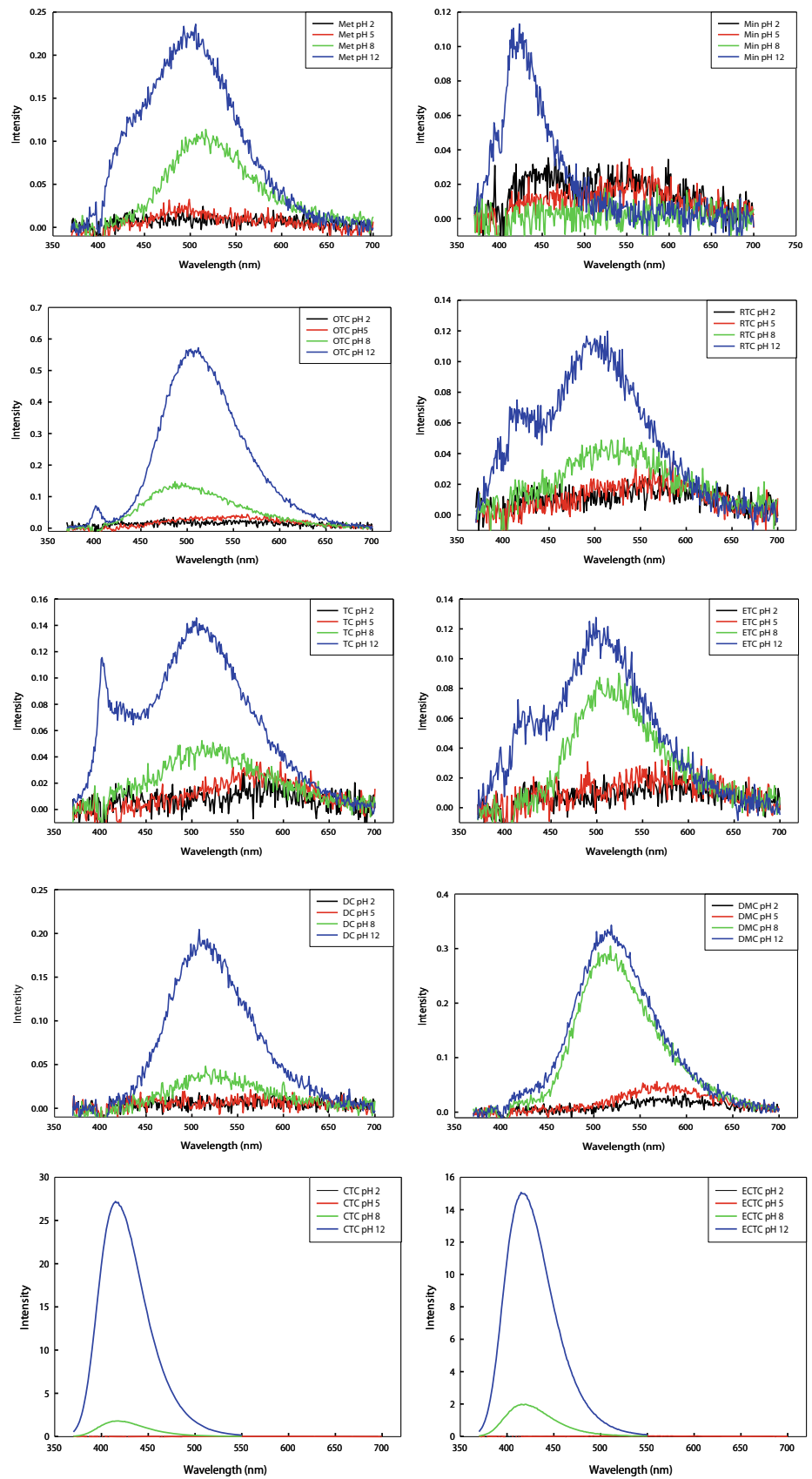


Fig. 3 pH dependent lowest energy absorbance maxima of different TCs. (TCs in 0.01 M buffer solutions)

Fig. 4 pH-dependent emission spectra each tetracycline. (λ_{ex} =335 nm for TCs in 0.01 M buffer solutions)



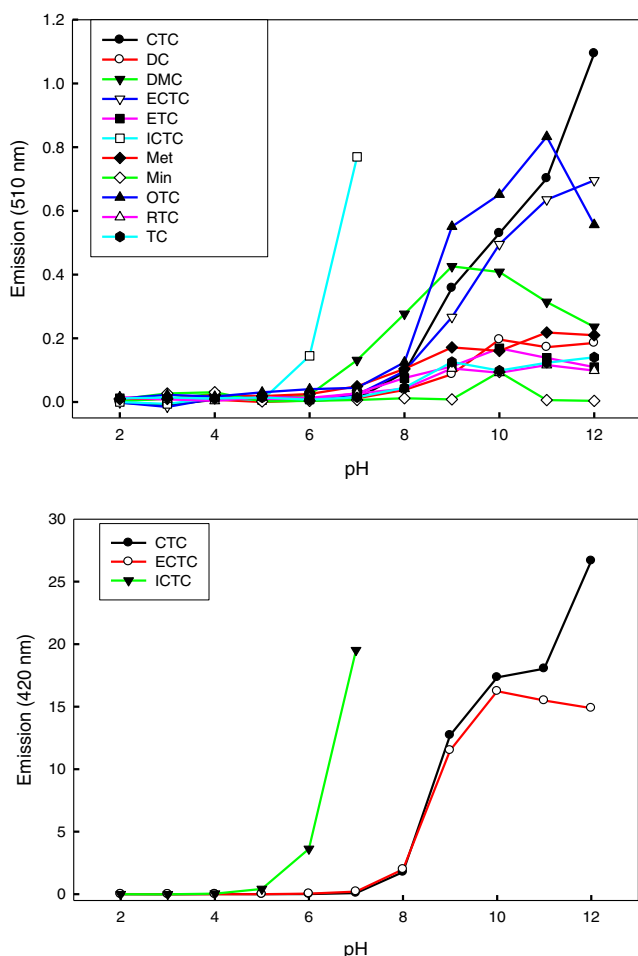
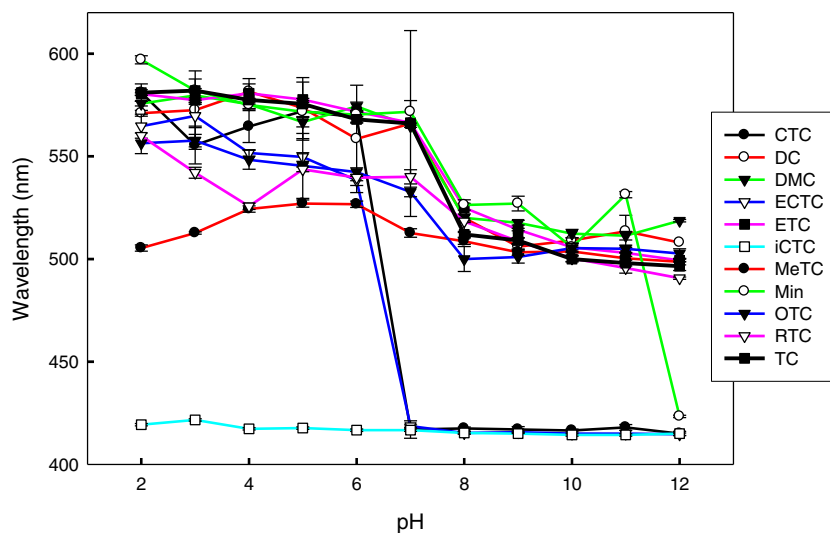


Fig. 5 pH-dependent intensity of the different tetracyclines. The emission of iCTC at >pH 7 is over the scale. ($\lambda_{\text{ex}}=335$ nm for TCs in 0.01 M buffer solutions)

Instrumentation The absorbance of all samples was recorded using a HP 8452A diode array spectrophotometer. Quartz cuvettes (1 cm^2) were used for all experiments.

Fig. 6 pH-dependent emission maxima of tetracyclines. ($\lambda_{\text{ex}}=335$ nm for TCs in 0.01 M buffer solutions)



Steady-state fluorescence spectra were recorded by using a SLM-AMINCO model 8100 using a 450 W Xe arc lamp as excitation source. The excitation wavelength used was 355 nm. The excitation and emission spectral band-passes were 4 nm. Emission spectra were background corrected by using appropriate blanks. The blank contribution was <2 % of the total emission for the experiments. All experiments were performed on at least three occasions.

Time-resolved fluorescence experiments were carried out by using an IBH model 5,000 W SAFE time-correlated single photon counting fluorescence lifetime instrument. An LED at 335 nm served as the excitation source. Single grating monochromators were used for wavelength selection. The count rate at each photomultiplier tube detector was kept below 2 % of the LED replication rate to avoid pulse-pileup. The experimental time resolution was 0.47 ns/channel. A 1024 MCA (multichannel analyzer) channels was used to record each decay trace, and data were acquired until there were at least 10,000 counts in the peak MCA channel for each decay trace.

The time-resolved intensity decay data from IBH was analyzed by using Globals WE (Globals Unlimited), a commercially available global analysis software package.

Results and Discussion

Electronic Absorbance Three distinct absorbance maxima (around 220, 270 and 360 nm) are observed in all samples except iCTC (Figs. 1 and 2). The bands are due to the presence of two chromophores namely the A chromophore, which comprises the β -tricarbonyl system of ring A and is responsible for the strong absorption at about 270 nm and the BCD chromophore, which comprises the π -electron system located on rings B, C and D and is responsible for all absorption

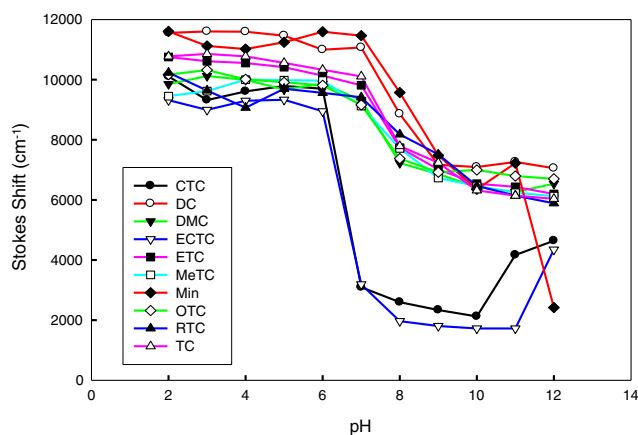


Fig. 7 pH-dependent Stokes shift of tetracycline analogs

maxima especially the strong visible band at 360 nm, which accounts for the TCs pale to bright yellow color [27, 28].

TC and its analogs exhibit similar pH-dependent absorbance spectra. All analogs are protonated at low pH values (2–3) and deprotonation at O3 occurs as pH increases leading to TCs zwitterionic form at pH 4–6. There is a slight red shift of the peak at 220 and 270 nm regions as pH increases. Further increase of pH above 7 or the dissociation of proton at O12 (above pK_{a2}) result in a bathochromic shift in the 360 nm region for these TCs [18, 25].

The absorbance in the 360 nm region is affected since deprotonation takes place at the BCD rings. Further increase of pH leading to the removal of proton at N4 results to changes not only in the 360 nm region (bathochromic shift) but also in the other regions. The characteristic bathochromic shift at 360 nm is due to the formation of anions due to the addition of base that resulted in a change in the geometry of the BCD chromophore [18, 25].

However, the three chlorinated TCs (CTC, ETC and iCTC) exhibit a behavior that is different from the other TC analogs (Fig. 2). At $pH > 7$, the absorbance of CTC and ECTC at the 360 nm decreases. Instead of a bathochromic shift at higher pH, a hypsochromic shift was observed at $pH > 7$. The changes in the absorbance spectrum also differ in comparison to the other TC analogs as an additional peak at 250 nm is observed at $pH > 10$. This behavior suggests only that CTC and ETC degrades to form a product. The reduction of absorbance around the 370 nm region could mean the rupture of one of

the ring leading to the formation of iCTC. On the other hand, iCTC showed no absorbance around the 360 nm region at $pH < 7$. An additional peak was found at the 360 nm region starting at pH 8 and by pH 11, identical absorbance profiles can be observed for ECTC, CTC and iCTC.

Figure 3 summarizes the absorbance maxima of the lowest energy band (360 nm) of TC and its analogs at different pH. Using TC as point of comparison, OTC, RTC and DC blue shifted at all pHs. The chlorinated TCs (CTC, ECTC and DMC) on the other hand, have their peak maxima at longer wavelength than TC at all pHs except for CTC which dropped starting at pH 11 and ECTC at pH 12. Meanwhile, peak maxima of lower wavelength than TC can be observed for MeTC (up to pH 7) and for Min (up to pH 9) that moved to longer wavelength than TC at higher pH. ETC, the epimer of TC, was found to have peak maxima at longer wavelength than that of TC.

The red and blue shift of the TC analogs with respect to TC is due to several factors, one of them is the functional group present in the BCD region. Addition of chlorine in the phenyl group caused the absorbance to red shift since it has been reported that substitution of a group containing a heteroatom like Cl results in the extension of the π -system [29]. For the ETC, it is possible that the epimerization at C4 is the main reason for the red shift.

For the analogs that blue shifted, only Min has a direct substitution in the phenyl ring. A dimethylamine was introduced in the phenyl ring and being an electron donating group, there is a rise in the π^* level relative to n level. Blue shift occurs in $n \rightarrow \pi^*$ transition resulting from the attachment of the electron donating group. Replacement of the hydroxyl group with a double bond in ring B in Met could be the reason for peak maxima to be in shorter wavelength. The same thing can be said to OTC and DC which has an additional hydroxyl group at ring B and the migration of hydroxyl group from ring C to ring B, respectively. Lastly, steric effect could account for the behavior of RTC. Although the one affected by RTC is the A chromophore; the bulk size of the functional group in amide is enough to have an effect on the BCD chromophore.

Steady-State Emission The effects of pH on the steady-state TC fluorescence are more significant in comparison to the electronic absorbance. In general, the fluorescence intensity

Fig. 8 Reversible reaction of CTC to iCTC at basic pH

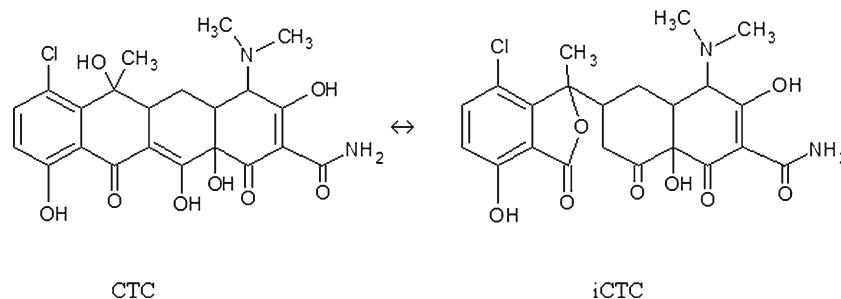


Table 2 pH dependent lifetimes and fraction of CTC, ECTC and iCTC

| | | χ^2 | Lifetimes (ns) | Fraction |
|-------|--------------------|----------|-------------------|------------------------|
| CTC | | | | |
| pH 7 | Single Exponential | 10.79 | 3.25 | |
| | Double Exponential | 1.78 | 4.34, 1.68 | 0.61, 0.39 |
| | Triple Exponential | 1.41 | 5.09, 2.38, 0.002 | 0.39, 0.61, 0.004 |
| pH 8 | Single Exponential | 9.11 | 4.31 | |
| | Double Exponential | 1.37 | 4.98, 1.58 | 0.81, 0.19 |
| | Triple Exponential | 1.00 | 5.19, 2.30, 0.05 | 0.71, 0.25, 0.04 |
| pH 9 | Single Exponential | 1.85 | 5.05 | |
| | Double Exponential | 1.16 | 5.12, 0.17 | 0.97, 0.03 |
| | Triple Exponential | 0.87 | 5.33, 2.97, 0.02 | 0.94, 0.05, 0.01 |
| pH 10 | Single Exponential | 1.70 | 5.26 | |
| | Double Exponential | 1.07 | 5.32, 0.17 | 0.98, 0.02 |
| pH 11 | Single Exponential | 1.11 | 5.26 | |
| | Double Exponential | 0.83 | 5.30, 0.06 | 0.98, 0.02 |
| pH 12 | Single Exponential | 1.11 | 5.22 | |
| | Double Exponential | 0.90 | 5.26, 0.005 | 0.996, 0.004 |
| ECTC | | | | |
| pH 7 | Single Exponential | 2.64 | 2.82 | |
| | Double Exponential | 1.38 | 5.56, 2.58 | 0.10, 0.90 |
| | Triple Exponential | 1.11 | 7.58, 2.74, 0.09 | 0.04, 0.93, 0.03 |
| pH 8 | Single Exponential | 4.16 | 3.06 | |
| | Double Exponential | 1.23 | 4.65, 2.43 | 0.31, 0.69 |
| | Triple Exponential | 1.03 | 5.22, 2.67, 0.03 | 0.19, 0.79, 0.02 |
| pH 9 | Single Exponential | 5.44 | 4.27 | |
| | Double Exponential | 1.21 | 4.96, 2.07 | 0.78, 0.22 |
| | Triple Exponential | 1.00 | 5.15, 2.64, 0.003 | 0.68, 0.32, 0.002 |
| pH 10 | Single Exponential | 2.34 | 4.88 | |
| | Double Exponential | 1.11 | 5.07, 1.44 | 0.94, 0.06 |
| pH 11 | Single Exponential | 1.49 | 5.05 | |
| | Double Exponential | 1.05 | 5.11, 0.23 | 0.98, 0.02 |
| pH 12 | Single Exponential | 1.21 | 5.03 | |
| | Double Exponential | 0.86 | 5.07, 0.08 | 0.98, 0.02 |
| iCTC | | | | |
| pH 7 | Single Exponential | 11.02 | 3.35 | |
| | Double Exponential | 1.57 | 4.28, 1.49 | 0.69, 0.31 |
| | Triple Exponential | 1.03 | 4.91, 2.39, 0.20 | 0.51, 0.44, 0.05 |
| pH 8 | Single Exponential | 9.04 | 4.38 | |
| | Double Exponential | 1.71 | 5.16, 1.70 | 0.79, 0.21 |
| | Triple Exponential | 1.36 | 5.60, 2.73, 0.19 | 0.61, 0.36, 0.03 |
| pH 9 | Single Exponential | 1.57 | 5.19 | |
| | Double Exponential | 1.01 | 5.26, 0.20 | 0.98, 0.02 |
| | Triple Exponential | 0.93 | 5.35, 2.26, 0.03 | 0.9513, 0.0354, 0.0133 |
| pH 10 | Single Exponential | 1.22 | 5.26 | |
| | Double Exponential | 0.89 | 5.30, 0.04 | 0.984, 0.02 |
| pH 11 | Single Exponential | 1.22 | 5.27 | |
| | Double Exponential | 0.82 | 5.31, 0.05 | 0.98, 0.02 |
| pH 12 | Single Exponential | 1.15 | 5.26 | |
| | Double Exponential | 0.88 | 5.30, 0.06 | 0.98, 0.02 |

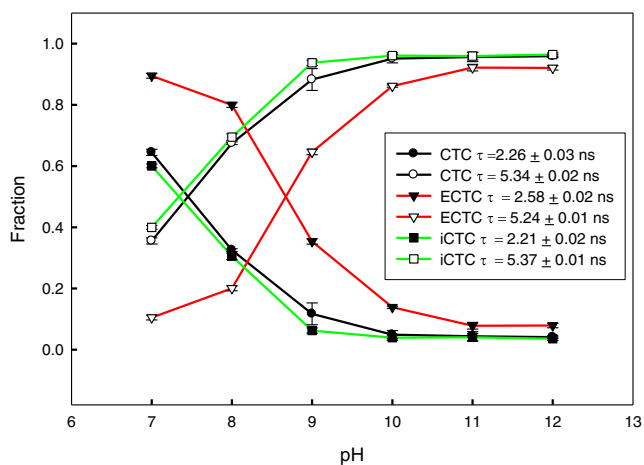


Fig. 9 Lifetimes fraction of CTC, ECTC and iCTC

increases as pH increases and the increase becomes more pronounced above pH 7 in all analogs (Fig. 4) with the exception of Min whose intensity decreases as pH increases. The emission intensity of the different TC analogs increases from pH 7 to pH 11 and began to drop by pH 12 which could be due rapid degradation of TCs [13].

These results confirm previous reports regarding TC and CTC being fluorescent at high pH. TC has been reported as a weakly fluorescent compound that became a highly fluorescent derivative when it binds to metals like Ca^{2+} and Mg^{2+} or in alkaline medium [30]. CTC, on the other hand, forms a highly fluorescent compound, iCTC, in basic solution [26, 31, 32]. No literature has yet reported the emission properties of the other TC analogs at different pH.

The peak maxima of most TC analogs shifted hypsochromically as the pH increases (Fig. 5). From an average peak maximum of 567 nm at pH 2, the average peak maximum at pH 12 was found at 484 nm. This blue shift was also observed in earlier studies like the one previously reported [18] wherein the peak maxima of tetracycline at 600 nm at

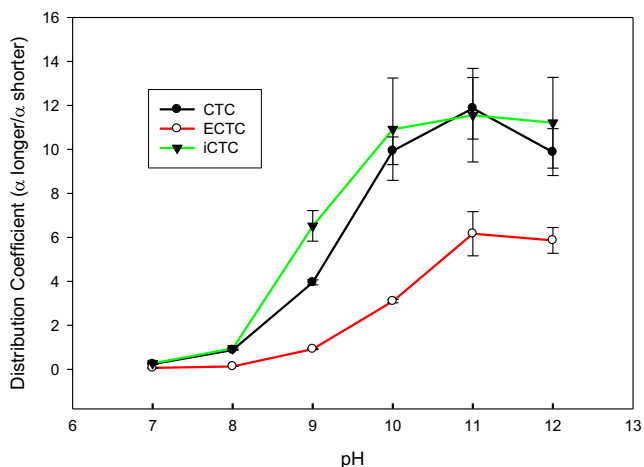


Fig. 10 pH-dependent distribution coefficient of CTC, ECTC and iCTC

low pH shifted to around 500 nm at high pH. For CTC and ECTC, the hypsochromic shift is much greater. The peak maxima shift from 580 nm at pH 2 to 420 nm at pH 7 (Fig. 6). In addition to the shift of peak maxima, an extra peak around 420 nm can be observed on TC, ETC, RTC and Met samples starting at pH 11 (pH 10 for TC). This is near the peak maxima of CTC. These peaks may correspond to the iso derivatives of said analogs which are also reported to be formed at higher pH although not as readily as the iCTC.

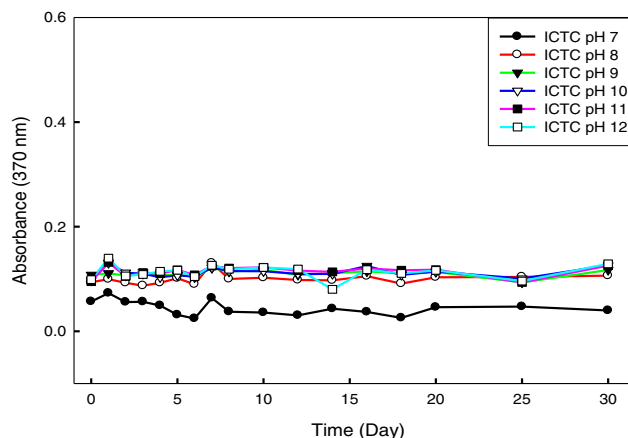
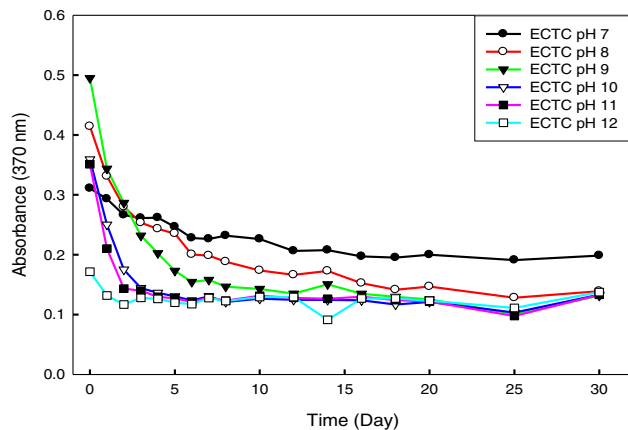
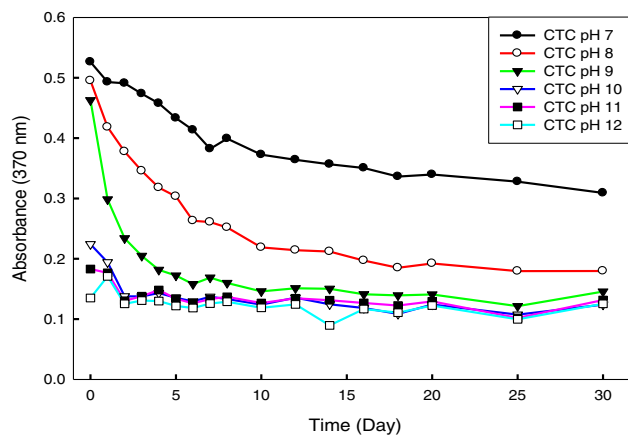


Fig. 11 Stability of CTC, ECTC and iCTC in basic pH

Fig. 12 Absorbance of CTC at different pH and different ionic strength [a]=0.001 M; [b]=0.01 M and [c]=0.1 M

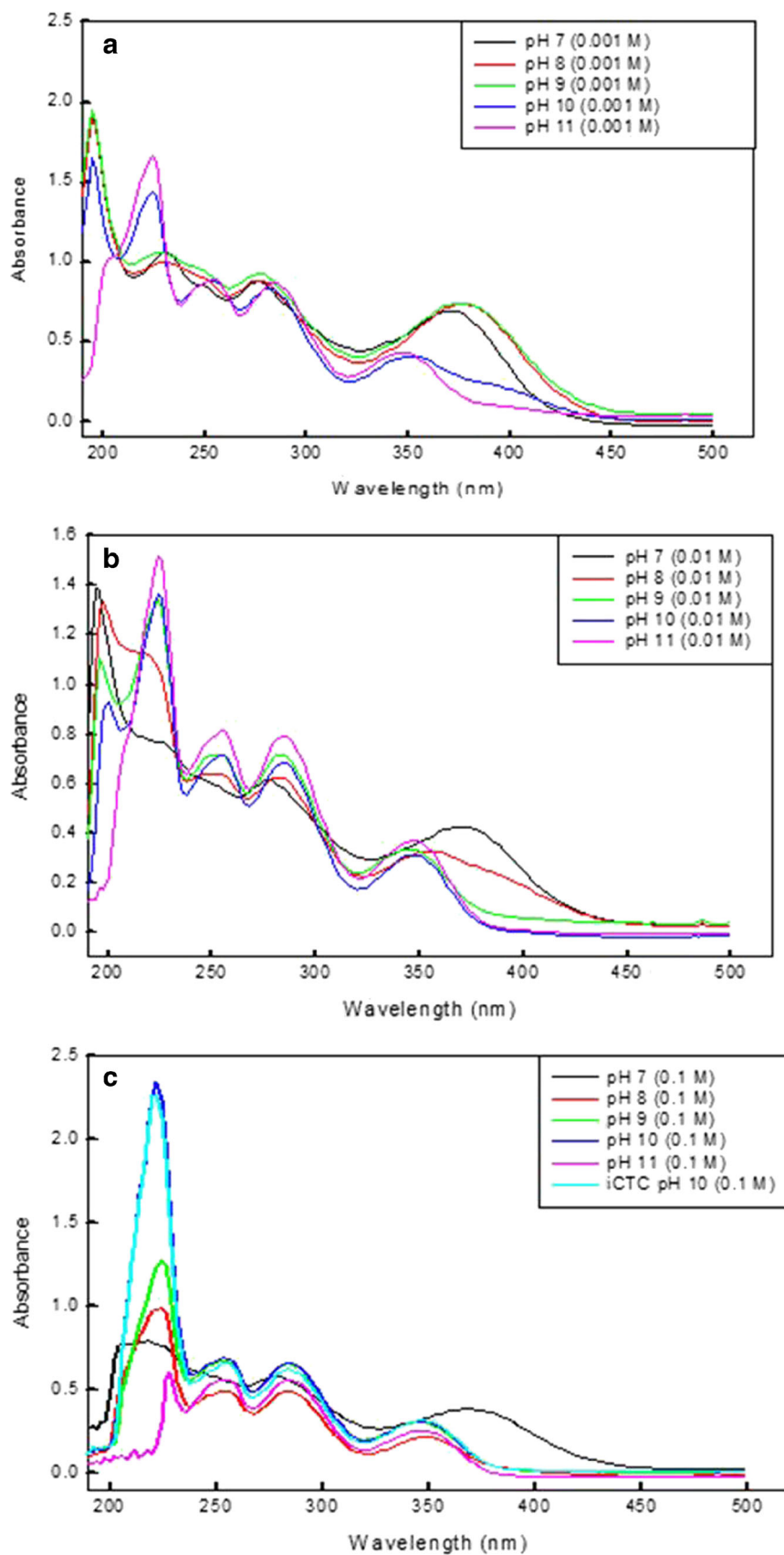
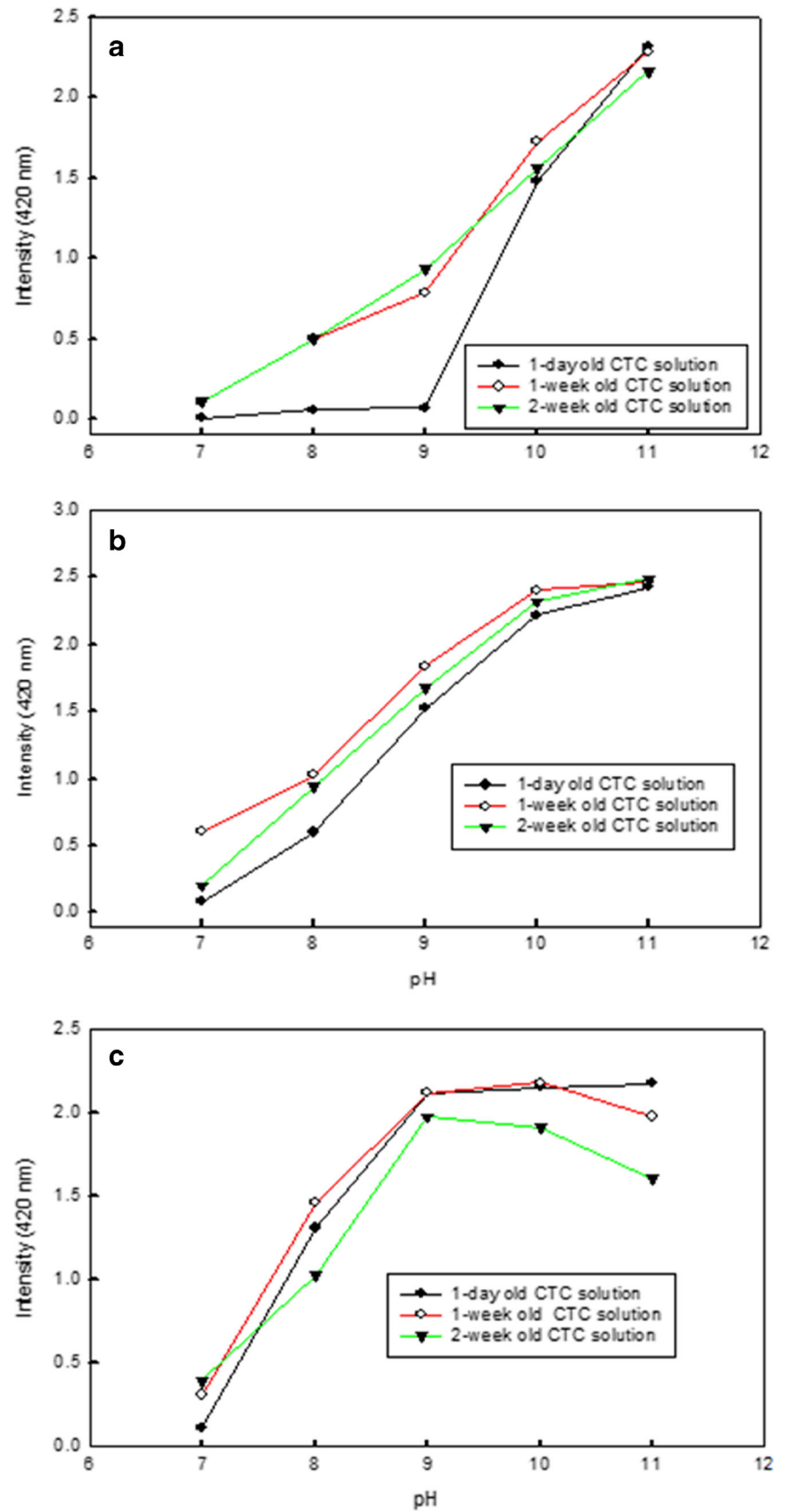


Fig. 13 Intensity at emission maxima (420 nm) of CTC at different pH and different ionic strength [a]=0.001 M; [b]=0.01 M and [c]=0.1 M. (λ_{ex} =335 nm)



Looking at the absorption spectra and the emission spectra of the analogs, a pH dependent Stokes shift is observed (Fig. 7). The excitation wavelength used is fixed at 355 nm and the absorption maxima is around 360 nm. At low pH, the emission maxima is around 580 nm and it shifts to around 500 nm at pH 12 and at the same time the absorption maxima

shifts to around 380 nm. The blue shift in the emission spectra and the red shift in the absorption as the pH increases resulted in a decrease of the gap between the absorption and emission maxima. This type of Stokes shift (large Stokes shift at low pH) is generally attributed to an adiabatic excited state intramolecular proton transfer (ESIPT) [16]. This phenomenon

Table 3 Lifetime of 50 μ M CTC at different pH and different ionic strength determined using TCSPC

| | | χ^2 | Lifetimes (ns) | Fraction |
|---------|--------------------|----------|-------------------|-------------------|
| 0.001 M | | | | |
| pH 7 | Single Exponential | 8.49 | 3.47 | |
| | Double Exponential | 1.28 | 4.32, 1.64 | 0.70, 0.30 |
| | Triple Exponential | 0.99 | 4.733, 2.34, 0.16 | 0.51, 0.45, 0.04 |
| pH 8 | Single Exponential | 11.14 | 4.22 | |
| | Double Exponential | 2.32 | 4.94, 1.17 | 0.81, 0.19 |
| | Triple Exponential | 1.92 | 4.99, 1.32, 0.018 | 0.79, 0.21, 0.002 |
| pH 9 | Single Exponential | 4.42 | 5.2 | |
| | Double Exponential | 1.13 | 5.56, 1.49 | 0.91, 0.09 |
| | Triple Exponential | 0.93 | 5.69, 2.43, 0.004 | 0.87, 0.13, 0.003 |
| pH 10 | Single Exponential | 1.74 | 5.65 | |
| | Double Exponential | 1.67 | 5.68, 0.03 | 0.99, 0.01 |
| pH 11 | Single Exponential | 1.55 | 5.5 | |
| | Double Exponential | 0.89 | 5.63, 1.20 | 0.97, 0.03 |
| 0.01 M | | | | |
| pH 7 | Single Exponential | 10.16 | 3.87 | |
| | Double Exponential | 1.29 | 4.83, 1.78 | 0.70, 0.30 |
| | Triple Exponential | 1.03 | 5.13, 2.38, 0.15 | 0.57, 0.39, 0.04 |
| pH 8 | Single Exponential | 5.15 | 5 | |
| | Double Exponential | 1.03 | 5.48, 1.70 | 0.867, 0.13 |
| | Triple Exponential | 0.88 | 5.61, 2.41, 0.03 | 0.81, 0.17, 0.02 |
| pH 9 | Single Exponential | 2.86 | 5.33 | |
| | Double Exponential | 1.02 | 5.66, 1.81 | 0.92, 0.08 |
| | Triple Exponential | 0.92 | 5.79, 2.81, 0.003 | 0.86, 0.14, 0.002 |
| pH 10 | Single Exponential | 1.43 | 5.54 | |
| | Double Exponential | 0.88 | 5.71, 1.65 | 0.96, 0.04 |
| pH 11 | Single Exponential | 1.42 | 5.58 | |
| | Double Exponential | 0.97 | 5.67, 0.71 | 0.98, 0.02 |
| 0.1 M | | | | |
| pH 7 | Single Exponential | 7.89 | 3.92 | |
| | Double Exponential | 1.16 | 4.77, 1.88 | 0.72, 0.28 |
| | Triple Exponential | 0.96 | 5.01, 2.43, 0.084 | 0.60, 0.37, 0.03 |
| pH 8 | Single Exponential | 3.3 | 5.17 | |
| | Double Exponential | 1.16 | 5.47, 1.54 | 0.92, 0.08 |
| | Triple Exponential | 1 | 5.58, 2.50, 0.11 | 0.88, 0.12, 0.002 |
| pH 9 | Single Exponential | 1.82 | 5.33 | |
| | Double Exponential | 1.01 | 5.50, 1.25 | 0.96, 0.04 |
| | Triple Exponential | 0.93 | 5.60, 2.70, 0.002 | 0.92, 0.08, 0.001 |
| pH 10 | Single Exponential | 1.14 | 5.36 | |
| | Double Exponential | 0.95 | 5.41, 0.15 | 0.99, 0.01 |
| pH 11 | Single Exponential | 1.4 | 5.36 | |
| | Double Exponential | 1.06 | 5.41, 0.19 | 0.98, 0.02 |

usually occurs when a proton acceptor ortho to the phenol group is present [33] just like the C11 keto group in TCs. The increased acidity of phenols in the excited singlet state is well known [34] and the resultant emission of the phenolate anion excited state generates a large Stokes shift. The red and blue shifts for TCs absorption and emission, respectively, occur usually near pH 8 when deprotonation at C10 or C12 (pK_{a2}) takes place. The red shift is said to come from the modest stabilization of the TC^- ground state in the resonance-delocalized anion while the blue shift of emission may be interpreted as an indication that the TC^- excited state decays radiatively via adiabatic transition directly to the ground state [16]. Although the behavior has been reported only for TC [16], it is also possible that ESIPT also occurs in other TC analogs because of the presence of C11 keto group. Although, there is also a large Stokes shift in CTC at low pH, ESIPT may not occur at basic pH because CTC is converted to iCTC [31, 32].

Time-Resolved Intensity Decays The strong fluorescence intensity exhibited by CTC at high pH was reported to arise from iCTC [31] (Fig. 8). The same behavior is anticipated for ECTC since ECTC can convert to CTC and then to iCTC with increase in pH. Time-resolved fluorescence intensity decay measurements of CTC, ECTC and iCTC between pH 7 and 12 were conducted to determine the component(s) present and responsible for the observed intensity behavior. The time-resolved fluorescence intensity decay gives more information on the nature of the fluorescing sample in comparison to a steady state experiment [35].

Results of this experiment are shown in Table 2. Inspection of the results in Table 2 shows that the triple exponential decay model with a chi-square (χ^2) close to unity is the best fit model for samples between pH 7 and 9. However upon closer examination of one of the obtained lifetime (0.002 ns) and amplitude (0.4 %), it is possible that the two-exponential decay model is the best fit. It is possible that the chi square value of the three exponential fit (1.41) is not statistically significant from the two exponential fit (1.78) since the chi square value itself has uncertainty [36]. Above pH 10, the intensity decays are best fit to single or double exponential models. The ~ 5 ns lifetime is assigned to iCTC because its contribution increases with increasing pH as iCTC is formed at higher pH.

These results suggest the presence of CTC and iCTC between pH 7 and 10 in the three samples. To explore the results further, we carried out a global analysis by simultaneously analyzing all the pH-dependent intensity decay traces for a given TC by linking the lifetimes across all pH and allowing the fractions, pre-exponential terms to float. The resulting global analysis (corrected for the blank) yielded two components with lifetimes around 2 and 5 ns close to the one observed earlier (Fig. 9). The contribution from the longer lifetime component increases as the pH increases while

the shorter lifetime component decreases. This is consistent with iCTC being formed from CTC at higher pH. This can be confirmed with the iCTC solution at the basic pH which has an almost identical graph as the CTC samples. With regards to the assignment of the lifetime, the longer lifetime is assigned to iCTC while the other one is assigned to CTC. For ECTC, it is converted to CTC at neutral pH and then to iCTC at basic pH. Results using ECTC showed that its conversion to iCTC is not the same as that of CTC. It is possible that CTC and iCTC are the components present in ECTC samples at basic pH.

In addition, the pH dependent distribution coefficient (ratio of the alpha of longer lifetime over the alpha of shorter lifetime or the fraction of the species with longer lifetime over the ratio of species with shorter lifetime) was determined. The CTC and iCTC samples showed almost the same values which could mean a pH dependent transformation between CTC and iCTC in comparison to ECTC (Fig. 10). For the ECTC as shown in Fig. 10 wherein freshly prepared samples were used, it is not converted readily to iCTC. It is transformed first to CTC and then to iCTC.

The stability of the three samples (stored at 4 °C) was also monitored by over a month period. Results are shown in Fig. 11 wherein the absorbance at 370 nm is plotted vs time. For the iCTC, there is no change in the absorbance with time. For CTC, there is a drop in the absorbance in pH 7 to 9 within the first few days and the same thing can be observed in ECTC where there is also a drop in the absorbance from pH 7 to pH 11 within the first few days. This indicates that CTC and ECTC undergo pH dependent transformation with time until a stable absorbance has been obtained.

Effect of Buffer Ionic Strength The buffers' ionic strength effect on the pH dependent transformation of CTC from pH 7 to 11 was also determined. Buffer concentrations of 0.1, 0.01 and 0.001 M were used to prepare 50 μ M CTC

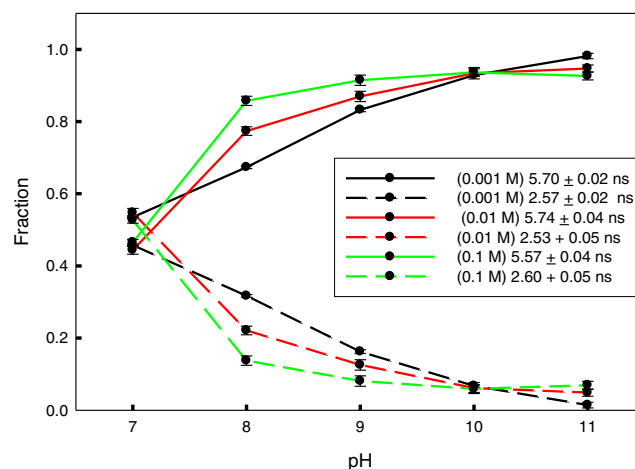


Fig. 14 Fractions of two lifetimes at different pH and different ionic strength

Table 4 Lifetime of 50 μ M iCTC (pH 10) at different ionic strength

| Time domain | | χ^2 | Lifetimes (ns) | Fraction |
|----------------|--------------------|----------|----------------|------------|
| iCTC (0.001 M) | Single Exponential | 4.21 | 5.23 | 1 |
| | Double Exponential | 1.06 | 5.61, 1.66 | 0.90, 0.10 |
| iCTC (0.01 M) | Single Exponential | 2.33 | 5.37 | 1 |
| | Double Exponential | 0.97 | 5.63, 1.69 | 0.93, 0.07 |
| iCTC (0.1 M) | Single Exponential | 1.28 | 5.49 | 1 |
| | Double Exponential | 0.95 | 5.53, 0.09 | 0.98, 0.02 |

solution. Yellow-greenish solution was observed on CTC solution at pH 7, 8 and 9 at 0.001 M buffer, pH 7 and 8 at 0.01 M and pH 7 at 0.1 M buffer. The ionic strength has an effect on the color of the CTC solution at basic pH. The higher the ionic strength, the less colored is the sample.

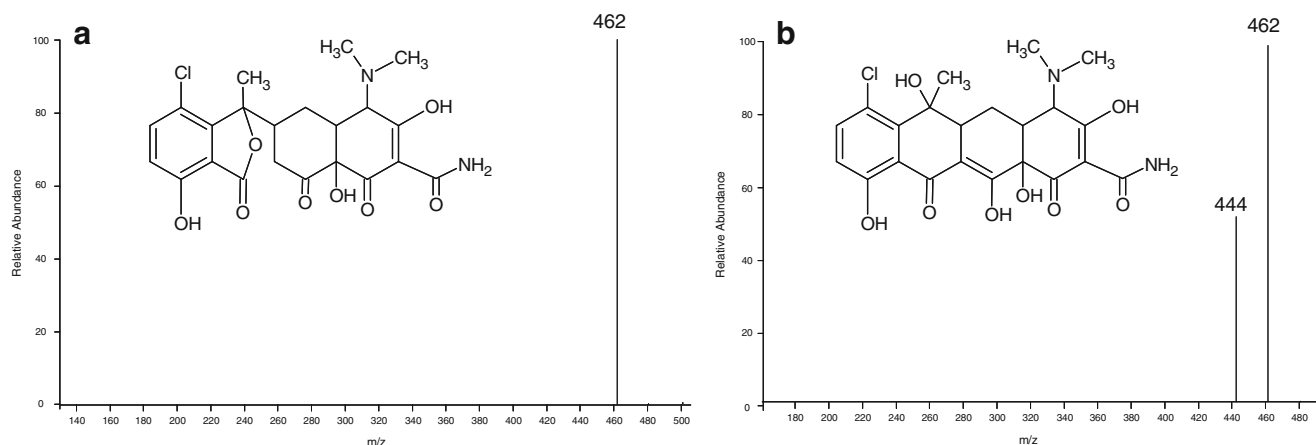
Figure 12 presents pH and ionic strength dependent absorbance of CTC. At the lowest ionic strength used (0.001 M), CTC at pH 7–9 has the same spectra around the 360 nm region. As the ionic strength increases to 0.1 M, only pH 7 has the same spectra around 360 nm region as before. The spectra of CTC at other pH decreases or somewhat deviate. This could only mean that as the ionic strength increases, CTC readily forms to iCTC. An iCTC solution at pH 10 gave the same spectra as the CTC at higher pH (Fig. 12c).

The emission property of CTC in basic solution was monitored at different aging time. Based on the results (Fig. 13), the fluorescence of CTC is dependent on the pH and buffer ionic strength. The higher the pH and the ionic strength, the more intense is the sample. However, when the ionic strength reached 0.1 M (Fig. 12c), the intensity began to flatten at pH 9–11. This could be due to the quenching of the ions that is present in high amount at 0.1 M. The strong intensity at higher pH is due to the formation of iCTC. The result in emission scan here just confirms the result obtained from the absorbance for the presence of iCTC.

To more fully evaluate this behavior, we determined the pH and ionic strength-dependent time-resolved fluorescence spectroscopy by using time correlated single photon counting (TCSPC) (Table 3). Two lifetimes (around 5 and 1–2 ns) are observed between pH 7 and 9. At pH 10 to 11, the single exponential is the best fit. To determine the fraction of each component at different pH, all the pH-dependent data sets were fit by to double exponential model and the lifetime were linked across the pH range. Global analysis fitted to double exponential was done wherein data panels from pH 7 to pH 11 were linked to one another. Results obtained are shown in Fig. 14. The one with the longer lifetime increases as the pH increases while the other one with shorter lifetime decreases. This could only mean that at higher pH, iCTC is the one present and assigned it with the longer lifetime. This is further supported when the lifetime of iCTC in pH 10 was also obtained. The obtained lifetime (Table 4) is near the longer lifetime (~5 ns). It also contained a higher fraction than the other lifetime obtained.

By comparing the fractions of lifetimes, a trend is observed wherein as pH increases, the higher the fraction of the longer lifetime. In addition, the higher ionic strength of the buffer also results in a higher fraction of the longer lifetime. All of this leads to confirmation of the assumption that CTC is readily converted to iCTC (Fig. 8) at higher pH and higher ionic strength. This is further supported by the mass spectrometric (MS) of the CTC in pH 10 at 0.1 M ionic strength which shows only one peak with a mass spectra pertaining to iCTC (Fig. 15). The MS/MS profile obtained for CTC is similar to the one reported by Farkas et al. [37].

Results from this study have a lot of theoretical and experimental implications especially in studies where TC and its derivatives are being used. Theoretical or computational studies on TC and its derivatives should always take into consideration the different forms that exist at different pH. There have been reported studies where TC and its derivative were used experimentally and compared with theoretical

**Fig. 15** MS/MS spectra of **a** iCTC and **b** CTC

calculations. Four TC derivatives (TC, OTC, RTC and DC) was assayed as potential flavivirus inhibitors and experimental and theoretical results showed that RTC and DC were able to show inhibitory effects [38]. However, it is not clear if the pH was taken into consideration in the study. The effect of pH may play an important role in the activity of the TCs used. The same thing can be applied on a study where experimental results using ELISA (enzyme linked immunosorbent assay) antibodies showed high relative affinity for TC and its derivatives and compared with computational calculations in terms of molecular static potentials and local average ionization energies and the role it plays in affecting the relative affinities of antibodies binding to TC compounds [39]. No consideration on the effect of pH was reported in this study. It is worthwhile to look on how the different forms of TC and its derivatives at different pH affect the results already reported.

Conclusions

The photophysics of 11 analogs of TC in different pH was determined. Most of the analogs exhibited the same absorbance signature with the presence of peaks at 220, 260 and 360 nm with the exception of iCTC which has no peak at 360 nm at acidic pH. Higher pH results in increased emission intensity in all TC analogs except minocycline. A pH dependent Stokes shift was observed and this type of Stokes shift (large Stokes shift at low pH) is generally attributed to an adiabatic excited state intramolecular proton transfer (ESIPT). The lifetime of CTC and iCTC was reported and the pH dependent transformation between the two was discussed.

Acknowledgments This material is based upon the work supported by the National Science Foundation (NSF) under Grant No. 0750321.

Any opinions and conclusion or recommendations expressed in this material are those of the author and do not necessarily reflect the views of the NSF. The author thanks Diana Aga of the Department of Chemistry, University at Buffalo for the use of the LC-MS instrument.

References

- Fernandez R, Dassie S (2005) Transfer of tetracyclines across the H₂O|1,2-dichloroethane interface: analysis of degraded products in strong acid and alkaline solutions. *J Electroanal Chem* 585:240–249
- Durckheimer W (1975) Tetracyclines: chemistry, biochemistry and structure-activity relations. *Angew Chem Int Ed* 14:721–734
- Schneider S (2001) Proton and metal ion binding of tetracyclines. In: Nelson M, Hillen W, Greenwald RA (eds) *Tetracyclines in biology, chemistry and medicine*. Birkhäuser, Basel, pp 65–104
- Stephens C, Murai K, Brunings K, Woodward R (1956) Acidity constants of the tetracycline antibiotics. *J Am Chem Soc* 78:4155–4158
- Asleson GL, Frank CW (1976) pH dependence of carbon-13 nuclear magnetic resonance shifts of tetracycline. Microscopic dissociation constants. *J Am Chem Soc* 98:4745–4749
- Leeson LJ, Krueger JE, Nash IA (1963) Concerning the structural assignment of the second and third acidity constants of the tetracycline antibiotics. *Tetrahedron Lett* 18:1155–1160
- Rigler NE, Bag SP, Leyden ED, Sudmeier JL, Reilly CM (1965) Determination of a protonation scheme of tetracycline using nuclear magnetic resonance. *Anal Chem* 37:872–875
- Garrett ER (1963) Variation of pK_a-values of tetracyclines in dimethylformamide-water solvents. *J Pharm Sci* 52:797–799
- Anand U, Jash C, Boddepalli RK, Shrivastava A, Mukherjee S (2011) Exploring the mechanism of fluorescence quenching in proteins induced by tetracycline. *J Phys Chem B* 115:6312–6320
- Chi Z, Liu R (2011) Phenotypic characterization of the binding of tetracycline to human serum albumin. *Biomacromolecules* 12:203–209
- Chi Z, Liu R, Yang H, Shen H, Wang J (2011) Binding of tetracycline and chlortetracycline to the enzyme trypsin: spectroscopic and molecular modeling investigations. *PLoS ONE* 6:e28361
- Choudhary S, Kishore N (2012) Unraveling the energetics and mode of the recognition of antibiotics tetracycline and rolitetracycline by bovine serum albumin. *Chem Biol Drug Des* 80:693–705
- Day S, Crouthamel W, Martinelli L, Ma J (1978) Mechanism of fluorometric analysis of tetracycline involve metal complexation. *J Pharm Sci* 67:1518–1523
- Jiang CQ, Wang T (2004) Study of the interactions between tetracycline analogues and lysozyme. *Bioorg Med Chem* 12:2043–2047
- Joseph K, Jun H, Luzzi L (1973) Tetracycline binding to bovine serum albumin studied by fluorescent techniques. *J Pharm Sci* 62:1261–1264
- Morrison H, Olack G, Xiao C (1991) Organic photochemistry. 93. Photochemical and photophysical studies of tetracycline. *J Am Chem Soc* 113:8110–8118
- Popov PG, Vaptzarova KI, Kossekova GP, Nikolov TK (1972) Fluorometric study of tetracycline-bovine serum albumin interaction. The tetracyclines - a new class of fluorescent probes. *Biochem Pharmacol* 21:2363–3672
- Schneider S, Schmitt MO, Brehm G, Reiher M, Matousek P, Towrie M (2003) Fluorescence kinetics of aqueous solutions of tetracycline and its complexes with Mg²⁺ and Ca²⁺. *Photochem Photobiol Sci* 2:1107–1117
- Mathew MK, Balam P (1980) A reinvestigation of chlortetracycline fluorescence: effect of pH, metal ions, and environment. *J Inorg Biochem* 13:339–346
- Li Z, Jiao G, Sun G, Song L, Sheng F (2012) Determination on the binding of chlortetracycline to bovine serum albumin using spectroscopic methods. *J Biochem Mol Toxicol* 26:331–336
- Ni Y, Liu Q, Kokot S (2011) Spectrophotometric study of the interaction between chlorotetracycline and bovine serum albumin using Eosin Y as site marker with the aid of chemometrics. *Spectrochim Acta A* 78:443–448
- Schlecht KD, Frank CW (1975) Dehydration of tetracycline. *J Pharm Sci* 64:352–354
- Doershchuk AP, Bitler BA, McCormick JRD (1955) Reversible isomerizations in the tetracycline family. *J Am Chem Soc* 77:4687
- Halling-Sørensen B, Sengeløv G, Tjørnelund J (2002) Toxicity of tetracyclines and tetracycline degradation products to environmentally relevant bacteria, including selected tetracycline-resistant bacteria. *Arch Environ Contam Toxicol* 44:7–16
- Mitscher LA (1978) *The chemistry of the tetracycline antibiotics*. Marcel Dekker, New York
- Waller CW, Hutchings BL, Wolf CF, Goldman AA, Broschard RW, Williams JH (1952) Degradation of aureomycin. VI. Isoaureomycin and aureomycin. *J Am Chem Soc* 74:4981
- Wessels JM, Ford WE, Szymczak W, Schneider S (1998) The complexation of tetracycline and anhydrotetracycline with Mg²⁺ and Ca²⁺: a spectroscopic study. *J Phys Chem B* 102:9323–9331

28. Siqueira J, Carvalho S, Paniago E, Tosi L, Beraldo H (1994) Metal complexes of anhydrotetracycline. 1. A Spectrometric study of the Cu(II) and Ni(II) complexes. *J Pharm Sci* 83:291–295
29. Appleton AL, Brombosz SM, Barlow S, Sears JS, Bredas JL, Marder SR, Bunz UHF (2010) Effects of electronegative substitution on the optical and electronic properties of acenes and diazaacenes. *Nat Commun* 1:91. doi:10.1038/ncomms1088
30. Sun XY, Chen H, Gao H, Guo XQ (2006) Screening of tetracyclines residues in fish muscles by CCD camera based solid-surface fluorescence. *J Agric Food Chem* 54:9687–9695
31. Blanchflower WJ, McCracken RJ, Rice DA (1989) Determination of chlortetracycline residues in tissues using high-performance liquid chromatography with fluorescence detection. *Analyst* 114:421–423
32. Feldman DH, Kelsey HS, Cavagnol JC (1957) Fluorometric determination of chlortetracycline. *Anal Chem* 29:1697–1700
33. Barbara PF, Jarzeba W (1988) Dynamic solvent effects on polar and nonpolar isomerizations. *Acc Chem Res* 21:195–199
34. Bartok W, Lucchesi PJ, Snider NS (1962) Protolytic dissociation of electronically excited organic acids. *J Am Chem Soc* 84:1842–1844
35. Lakowicz JR (2006) Principles of fluorescence spectroscopy, 3rd edn. Springer, New York
36. Andrae R, Schulze-Hartung T, Melchior P (2010) Dos and don'ts of reduced chi-squared. arXiv:1012.3754
37. Farkas M, Mojica E, Patel M, Aga D, Berry J (2009) Development of a rapid biolistic assay to determine changes in relative levels of intracellular calcium in leaves following tetracycline uptake by pinto bean plants. *Analyst* 134:1594–1600
38. Yang JM, Chen YF, Tu YY, Yen KR, Yang YL (2007) Combinatorial computational approaches to identify tetracycline derivatives as flavivirus inhibitors. *PLoS ONE* 5:e428
39. Kulshretha P, Sukumar N, Murray JS, Giese RE, Wood TD (2009) Computational prediction of antibody binding sites on tetracycline antibiotics: electrostatic potentials and average local ionization energies on molecular surfaces. *J Phys Chem A* 113:756–766